Available online at www.sciencedirect.com
ScienceDirect
Biosensors and Bioelectronics 23 (2008) 1610–1615
BIOSENSORS & BIOELECTRONICS
www.elsevier.com/locate/bios

Direct electrochemistry of cytochrome *c* at ordered macroporous active carbon electrode

Lei Zhang *

Department of Chemistry, College of Life and Environment Sciences, Shanghai Normal University, Guilin Road 100, Shanghai 200234, China

Received 15 September 2007; received in revised form 22 January 2008; accepted 25 January 2008
Available online 5 February 2008

Abstract

Three-dimensionally (3D) ordered macroporous active carbon has been fabricated and used as electrode substrate for the direct electrochemistry of horse heart cytochrome *c* (Cyt *c*). The Cyt *c* immobilized on the surface of the ordered macroporous active carbon shows a pair of well-defined and nearly reversible redox waves at the formal potential of −0.033 V in pH 6.8 phosphate buffer solution. The interaction between Cyt *c* and the 3D macroporous active carbon makes the formal potential shift negatively compared to that of Cyt *c* in solution. Spectrophotometric and electrochemical methods have been used to investigate the interaction between Cyt *c* and the porous active carbon. The immobilized Cyt *c* maintains its biological activity, and shows a surface controlled electrode process with the electron-transfer rate constant (k_s) of 17.6 s^{-1} and the charge-transfer coefficient (*a*) of 0.52, and displays the features of a peroxidase in the electrocatalytic reduction of hydrogen peroxide (H_2O_2). A potential application of the Cyt *c*-immobilized porous carbon electrode as a biosensor to monitor H_2O_2 has been investigated. The steady-state current response increases linearly with H_2O_2 concentration from 2.0×10^{-5} to 2.4×10^{-4} mol l^{-1}. The detection limit (3σ) for determination of H_2O_2 has been found to be 1.46×10^{-5} mol l^{-1}.
© 2008 Published by Elsevier B.V.

Keywords: Ordered macroporous carbon; Cytochrome *c*; Hydrogen peroxide; Direct electrochemistry

1. Introduction

Due to the highly ordered porous structure, large surface area, and tight pore size distributions, three-dimensionally ordered macroporous materials have been used widely in separation, catalysis, optical information processing and microwave shielding (Yablonovitch, 1987; Xia et al., 2000; Velev and Kaler, 2000). These porous materials, such as mesoporous silicate materials (MPS), are also very suitable as hosts for large organic molecules (Johnson et al., 1999) and proteins (Washmon-Kriel et al., 2000; He et al., 2000). Owning to their stability, and easiness to be modified with various functional groups, which can enable the electrostatic attraction or repulsion between porous materials and the proteins of interest to be studied (Han et al., 1999), some porous materials have been used as supports for immobilizing enzymes (He et al., 2000; Han et al., 1999; Díaz and Balkus, 1996) and applied in biosensors (He et al., 2000), biocatalytic (Díaz and Balkus, 1996), and biomolecule separation systems (Han et al., 1999). For example, Han et al. (1999) have used MPS to sequester and release proteins of similar size but varying charge, Díaz and Balkus (1996) have used MPS to immobilize Cyt *c*, Deere et al. (2001) have studied the adsorption isotherms for Cyt *c* onto MPS with different pore sizes, and also the peroxidative activity profiles of the adsorbed Cyt *c*, and Dimakis et al. (2002) have fabricated stable biosensors using macroporous carbon as matrix for the immobilization of polyelectrolyte-stabilized enzymes with high operational stability and good sensor-to-sensor reproducibility. Recently, Lei et al. (2001) have fabricated well-ordered 3D macroporous active carbon by carbonizing an aqueous solution of sucrose in the presence of sulfuric acid without use of any surfactants.

Cyt *c* plays an important role in the biological respiratory chain, whose function is to receive electrons from Cyt *c* reductase and deliver them to Cyt *c* oxidase. Thus, it is important to study the electrochemical behavior of Cyt *c*. Since the first

* Tel.: +86 21 64322270.
E-mail addresses: chemzl@shnu.edu.cn, chmzhanglei@gmail.com.

0956-5663/$ – see front matter © 2008 Published by Elsevier B.V.
doi:10.1016/j.bios.2008.01.022

electrochemical study of Cyt *c* at a gold electrode with a promoter 4,4′-bipyridyl was reported in 1977 (Eddowes and Hill, 1977), many other compounds have been used to promote the electron transfer of Cyt *c* on electrode surfaces (Taniguchi et al., 1982, 1984; Barker et al., 1990; Santucci et al., 1991). To employ the electrostatic attractions, carboxylic acid-terminated alkanethiols have been used as electrode modifiers and thus Cyt *c* was electrostatically adsorbed onto the modified layer. The Cyt *c* adsorbed in this way could be remained in its native form and exhibited redox peaks (Tarlov and Bowden, 1991; Song et al., 1993; Feng et al., 1995; Jin et al., 1997).

On the other hand, the extensively studied carbon material, including the forms of paraffin-impregnated spectroscopic graphite (Brabec et al., 1982) highly oriented pyrolytic graphite (Strauss et al., 2004; Burrows et al., 1991), glassy carbon (Liu et al., 2006; Hagen, 1989), and carbon nanotubes (Wang et al., 2002; Zhao et al., 2005; Wu and Hu, 2005), has also been widely used to promote the electron-transfer reaction of Cyt *c*. This is based on the high electron conductivity, better chemical stability, and the oxygen-containing functionalities on the carbon surface. Recently, Zhao et al. (2005) fabricated a multi-walled carbon nanotubes (MWNT) modified glassy carbon electrode for the direct electrochemical investigation of Cyt *c*, a couple of well-defined and quasi-reversible cyclic voltammetry peaks of Cyt *c* have been obtained in a phosphate buffer solution (pH 7.0). This indicates that MWNT can be used as a mediator for improving electron transfer of Cyt *c*.

Elicited by the potential practicability of carbon with porous structure, in this report, 3D ordered macroporous active carbon has been fabricated and used to study the electrochemical behavior of Cyt *c*. Field emission scanning electron microscope (SEM), transmission Fourier transform infrared (FT-IR) spectra and electrochemical technique have been employed to characterize the as-prepared electrodes. The aim of the present study is to investigate the immobilization of Cyt *c* on/inside the 3D ordered macroporous active carbon and thereafter the direct electron transfer between Cyt *c* and carbon. And, it is also intended to know the electroactivity of Cyt *c* immobilized on the surface of the 3D ordered macroporous active carbon and its pseudo peroxidase activity.

2. Experimental

2.1. Chemicals and solutions

Horse heart cytochrome *c* (Sigma) was prepared in 5 mmol/l phosphate buffer solution (PBS, pH 6.8). Sucrose was purchased from Sigma and used as received, H_2SO_4 (98%) was obtained from Shanghai Chemical Reagents Company (Shanghai). Monodispersed colloidal particles of silica (aqueous dispersions, 100 nm–1 μm in diameter) were obtained from Nissan Chemical Industries (Tarrytown, NY). All other chemicals were of analytical grade and used as received.

All experiments were made at room temperature (≈26 °C) unless stated otherwise. The solutions were thoroughly deoxygenated by bubbling highly purified nitrogen and a nitrogen atmosphere was maintained over the solutions.

2.2. Apparatus

All electrochemical experiments were performed on a CHI 660A electrochemical analyzer (USA) in a three-electrode electrochemical cell using 3D ordered macroporous active carbon as working electrode, twisted platinum wire as auxiliary electrode, and a saturated calomel electrode (SCE) as reference electrode.

A JXA 840 field emission scanning electron microscope (SEM, JEOL, Japan) was used to examine the morphologies of the 3D ordered macroporous active carbon. Transmission Fourier transform infrared (FT-IR) spectra were obtained by using a Nicolet 520 (Nicolet, USA) spectrophotometer in the range between 4000 and 400 cm^{-1}, at a spectral resolution of 4 cm^{-1} with an average of 128 spectral scans accumulated; KBr powder (Aldrich, USA) was used as both a diluent and for the background spectra. All samples were dispersed in KBr at ratios of between 5 and 10%; after each sample was ground together with the appropriate quantity of KBr carefully, the mixture of sample and KBr was pressed into a pellet for testing.

2.3. Electrode preparation

2.3.1. Preparation of the 3D ordered macroporous active carbon

3D ordered macroporous carbon was fabricated according to the reported procedure (Lei et al., 2001). Briefly, about 2 g SiO_2 template was added to a solution containing 2.5 g sucrose, 0.15 ml H_2SO_4 (98%) and 10 ml distilled water. The mixture was firstly heated at 100 °C for 6 h, then followed by heating at 150 °C for another 6 h. Complete carbonization was accomplished by heating the above composite in a tube oven in vacuo at 850 °C for 2 h. The residual surface carbon was removed from the composite and the SiO_2 template was then etched away by overnight dissolution in 10% aqueous HF solution to leave behind a highly ordered macroporous active carbon. Elemental analysis (C, 97.1, Si, 0.12%) indicates that this treatment removes almost all the SiO_2 template and thus high-quality macroporous active carbon is obtained. The structure of the obtained 3D macroporous active carbon has been characterized by scanning electron microscopy (Fig. 1). As can be seen, a regular hexagonal structure is clearly observed, and the next lower layer can also be seen in the high magnification image (inset of Fig. 1). The small dark areas within each pore are the interconnected necks formed during the sintering and correspond to the points of contact of the starting SiO_2 spheres.

2.3.2. Fabrication of 3D ordered macroporous carbon electrode

Firstly, a piece of 3D ordered macroporous carbon was carefully cut into a round disk with diameter of 2.8 mm and thickness of 3.2 mm, the disk was then squeezed into polytetrafluoroethylene (PTFE) thin film tube, and a copper rod was put into the PTFE thin film tube from the opposite and contacted with the 3D ordered macroporous carbon with silver conducting paint. Finally, the copper rod and the affixed 3D ordered macroporous carbon was tightly sealed by the outer PTFE thin film tube by heating under infrared light for a few minutes.

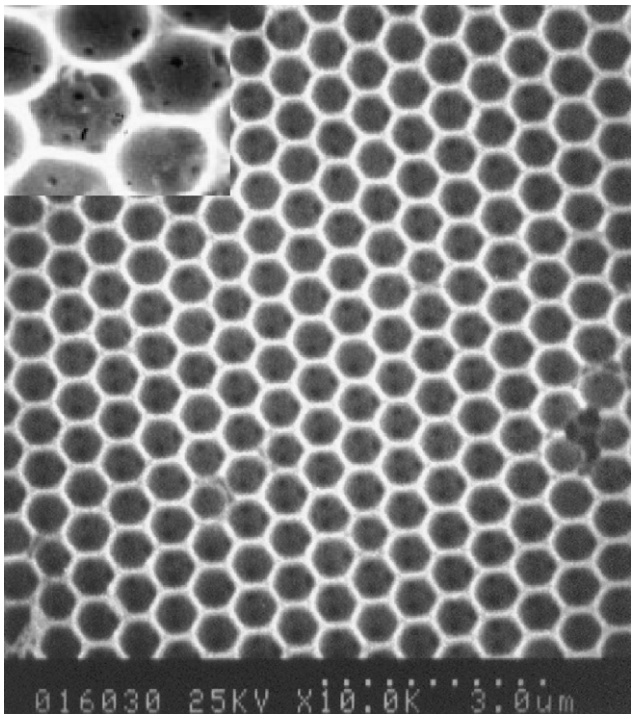

Fig. 1. SEM images of the ordered structure of the macroporous active carbon. Inset: SEM image of the macroporous active carbon with higher magnification.

To further activate the 3D ordered macroporous carbon and have more oxygen-containing functionalities, especially of carboxylic oxygen groups, on the surface of the porous active carbon, the 3D ordered macroporous carbon electrode (MPCE) was pre-anodized by polarizing it in 0.15 mol l^{-1} H_2SO_4 at 1.8 V for 5 min. It is known that the chemical and electrochemical treatment of carbon electrodes in oxidizing reagents can generate oxygen-containing functional groups, such as carbonyl, quinoid, carboxylate and hydroxyl radical species on the surface of carbon, and the phenolic oxygen and carboxylic oxygen are the important ones as derived from the XPS results (Cabaniss et al., 1985). These functional groups can accelerate or electrocatalyse irreversible oxidation of some organic compounds (Mattson and Mark, 1971).

3. Results and discussion

3.1. Characterization of the activated MPCE

Fig. 2A shows the cyclic voltammograms (CV) of the activated MPCE in 0.1 mol l^{-1} PBS (pH 6.8). It can be seen from this figure that MPCE exhibits a pair of redox peaks at the potentials of −0.067 and −0.105 V, respectively. This is due to the reduction and re-oxidation of carboxylic acid groups, which has been verified by FT-IR spectra (Fig. 3). The curve *a* in Fig. 3 shows the spectrum of the oxidized MPCE, the bands centered at 2944.2, 2708.8 and 2556.4 cm^{-1} are assigned to the O–H stretch of the hydroxyl groups in the carboxylic groups. The strong and sharp band at 1715.8 cm^{-1} is characteristic of carboxylic carbonyl groups. The bands centered at 1379.6 and 1195.4 cm^{-1} may be assigned to the stretching modes of C–O

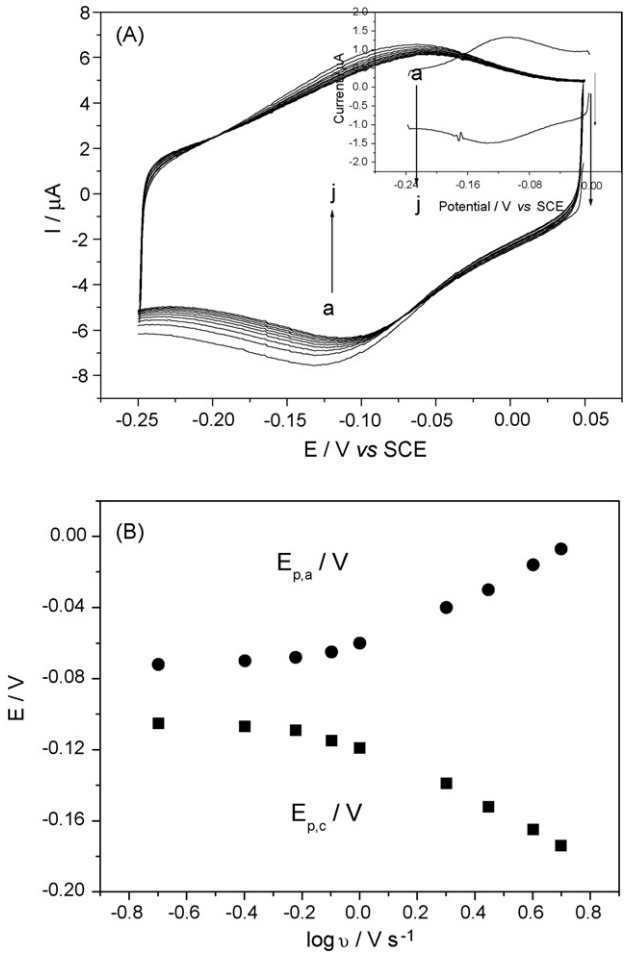

Fig. 2. (A) Consecutive CVs of the activated MPCE in 0.1 mol l^{-1} PBS (pH 6.8) at 0.1 V s^{-1} and (B) variation of peak potential vs. the logarithm of scan rate. Inset of A: CV of MPCE in 0.1 mol l^{-1} PBS (pH 6.8) at 0.02 V s^{-1}.

bonds in the $–COO^-$ groups as a consequence of the dissociation of the carboxylic acid functionalities. Bands at 1052.3, 837.1 and 673.5 cm^{-1} possibly indicate the O–H bending vibrations of the hydroxyl groups. And, the curve *b* in Fig. 3 shows the spec-

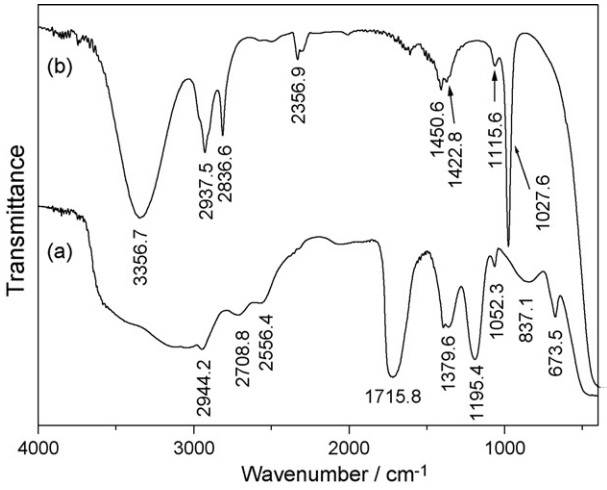

Fig. 3. FT-IR spectra of oxidized (curve *a*) and reduced (curve *b*) forms of MPCE.

trum of the reduced MPCE. As can be seen, the band centered at 3356.7 cm^{-1} is assigned to the O–H stretch of hydroxyl groups. The two bands at 2937.5 and 2836.6 cm^{-1} are characteristic of the stretching modes of C–H bonds in methylene. The bands at 1450.6 and 1422.8 cm^{-1} are assigned to the O–H bending vibrations of the hydroxyl groups. The next two bands at 1115.6 and 1027.6 cm^{-1} are attributed to the stretching vibrations of C–O bonds. These results show that the electroactive component on the surface of MPCE may be the carboxylic acid functionalities, which can be reduced to hydroxyl groups with a four-electron reduction process.

To further investigate the mechanism of the four-electron reduction of carboxylic acid groups, the effect of scan rate on the voltammetric behavior of MPCE was studied in detail. Fig. 2B shows the relationship between peak potential (E_p) and the logarithm of scan rates (υ) for MPCE in 0.1 mol l^{-1} PBS (pH 6.8) at different scan rates. As can be seen, with increasing scan rate the oxidation wave shifts to more positive potential, while the reduction wave shifts to more negative potential. The anodic and catholic peak potentials were linearly dependent on log υ when $\upsilon > 2.0$ V s^{-1}, which was in agreement with the Laviron theory (Laviron, 1979): a graph of $E_p = f(\log \upsilon)$ yields two straight lines with a slope equal to $-2.3RT/\alpha nF$ for the cathodic peak, and $2.3RT/(1-\alpha)nF$ for the anodic peak (Fig. 2B), so that a value of 0.49 can be determined for the charge-transfer coefficient (α) from the slope of the straight lines based on the equation:

$$\log \frac{k_a}{k_c} = \log \left[\frac{\alpha}{(1-\alpha)}\right] \quad \text{or} \quad \frac{k_a}{k_c} = \frac{\alpha}{1-\alpha} \tag{1}$$

where k_a (0.083) is the slope of the line derived from $E_{p,a} = f(\log \upsilon)$; k_c (0.087) is the slope of the line derived from $E_{p,c} = f(\log \upsilon)$; α is the charge-transfer coefficient. The apparent electron-transfer rate constant (k_s) for electron transfer between the electrode and the surface deposited layer can also be estimated to be (5.1 ± 0.2) s^{-1} according to the following equation ($\upsilon > 2.0$ V s^{-1}):

$$\log k_s = \alpha \log(1-\alpha) + (1-\alpha)\log \alpha - \log\left(\frac{RT}{nF\upsilon}\right) - \frac{\alpha(1-\alpha)nF\,\Delta E_p}{2.3\,RT} \tag{2}$$

when $\upsilon \to 0$, both the cathodic and anodic peaks tend towards the "reversible peaks", which are symmetrical with respect to the potential axis, and shows a nearly symmetrical shape (inset of Fig. 2A), the width (88.1 mV) at mid-height $\delta_{0.5}$, which becomes independent of α, tends towards $90.6/n_a$ mV (Laviron, 1979), so that $n_a = 1.03 \approx 1$, indicating that the rate determining step (r.d.s.) in the whole electrode process was a one-electron reduction process (Baizer and Lund, 1983).

MPCE shows a rather stable CV response in PBS (pH 6.8), as illustrated in Fig. 2A. It can be seen that the cathodic peak potential shows a slightly positive shift during the first five scans, and then keeps unchanged for further potential-scanning, while the anodic peak potential keeps almost unchanged for the continuous scans. The redox peak current shows a slight decrease during the first five cycles, and then keeps stable after five cycles. After 10 continuous scans, the electrode was rinsed successively with water and ethanol, and stored in the air at room temperature for 1 day. The electrode was then treated again by cyclic scanning under the same conditions. The peak potentials and current responses remained unchanged, indicating that MPCE was very stable.

3.2. Immobilization and electrochemical behavior of Cyt c at MPCE

To investigate the potential use of the 3D ordered macroporous active carbon in practice, the immobilization and electrochemical characteristics of Cyt *c* at MPCE have been investigated in detail.

To immobilize Cyt *c* on the surface of MPCE, MPCE was immersed into 5 mM PBS pH 6.8 containing 0.5 mM Cyt *c* and kept in a refrigerator for 16 h. During this period the Cyt *c* was spontaneously adsorbed on the surface of MPCE. Then, the immersed MPCE was rinsed with water to get ride of the non-firmly adsorbed Cyt *c* molecules. Thus, the Cyt *c* modified MPCE (Cyt *c*/MPCE) was obtained.

To confirm the immobilization and the electroactivity of Cyt *c* on the surface of MPCE, the Cyt *c*/MPCE was put in 5 mM PBS (pH 6.8) for cyclically potential-scanning (Fig. 4). It can be seen from Fig. 4A (curve *a*) that a pair of redox peaks appear with the formal potential of −0.033 V for the redox reaction of Cyt *c*, which is negatively shifted compared to that of Cyt *c* in solution ($E^{\circ\prime} = 0.017$ V) (Hawkridge and Kuwana, 1973), indicating the presence of interaction between Cyt *c* and the 3D ordered macroporous active carbon. This interaction may occur from the electrostatic interaction between positively charged Cyt *c* (p*I* = 10.5) (Jiang et al., 2004) and negatively charged carboxylic groups on the surface of MPCE and the intercalation interaction of Cyt *c* with the 3D porous active carbon itself. This indicates that MPCE can capture Cyt *c* from solution via adsorption and intercalation. However, one cannot observe the redox peaks of MPCE itself in Fig. 4; this can be assumed that the presence of Cyt *c* on carbon surface restrains the electrochemical activity of carbon material, which needs to be further investigated.

The interaction between the positively charged Cyt *c* and the negatively charged MPCE can also be confirmed by spectral characterization. Fig. 5 shows the FT-IR absorption spectra of native Cyt *c* (dotted line) and that of Cyt *c* after being interacted with 3D porous active carbon (solid line). As can be seen from Fig. 5 that, after being immobilized by 3D porous carbon, the absorption peaks of Cyt *c* observed at 1647.9, 1556.6, 1462.4 and 1407.0 cm^{-1} are shifted to 1657.6, 1545.5, 1448.6 and 1402.8 cm^{-1}, respectively. This result indicates the presence of the electrostatic and/or the intercalation interaction between positively charged Cyt *c* and negatively charged 3D porous carbon; these interactions had influenced the electron states and the spectroscopic properties of Cyt *c* to some extent. It can be assumed that these interactions enhanced the adsorption/binding and therefore the immobilization of Cyt *c* on the 3D porous carbon surface.

To further investigate the characteristics of Cyt *c* adsorbed on the surface of MPCE, the effect of scan rates on the voltammetric behavior of Cyt *c* was studied in detail. Fig. 4 shows the

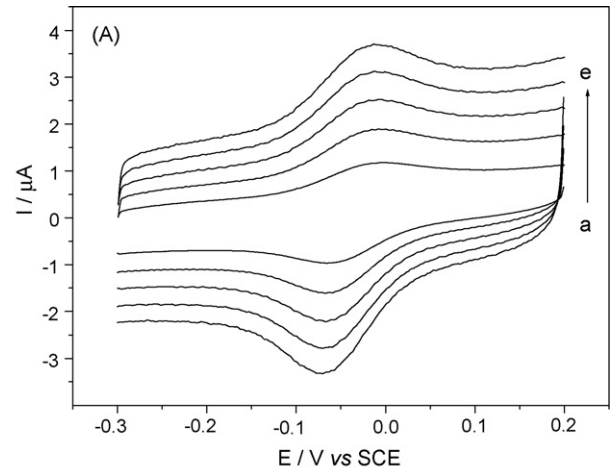

Fig. 4. (A) and (B) CVs of Cyt *c*/MPCE at different scan rates in 0.1 mol l^{-1} PBS (pH 6.8). Scan rates from (a) to (r) are 0.2, 0.4, 0.6, 0.8, 1.0, 1.0, 1.5, 2.0, 2.5, 3.0, 3.5, 4.0, 4.5, 5.0, 5.5, 6.0, 6.5, 7.0 V s^{-1}, respectively.

CVs of Cyt *c*/MPCE in 5 mM PBS (pH 6.8) at different scan rates. It can be seen that the redox peak current increases linearly with scan rates, which indicates that the redox process is confined to the surface of MPCE, confirming that the immobilized state of Cyt *c* is stable. On the other hand, it can be seen that, with increasing of scan rates, the oxidation peak shifts to more positive potentials, while the reduction peak shifts to more negative potentials. The anodic and cathodic peak potentials are linearly dependent on log υ when $\upsilon > 1$ V s^{-1}, according to the Laviron theory (Laviron, 1979) and the relationship between E_p and log υ, α and k_s can be estimated as 0.52 and 17.6 s^{-1} based on Eqs. (1) and (2), respectively. The k_s value is higher than some of the previously reported k_s values (0.7–14 s^{-1}) (Collinson et al., 1992; Tarlov and Bowden, 1991; Ju et al., 2002; Huang et al., 1996), which indicates that the Cyt *c* immobilized on MPCE surface shows good reversibility of the electron-transfer process.

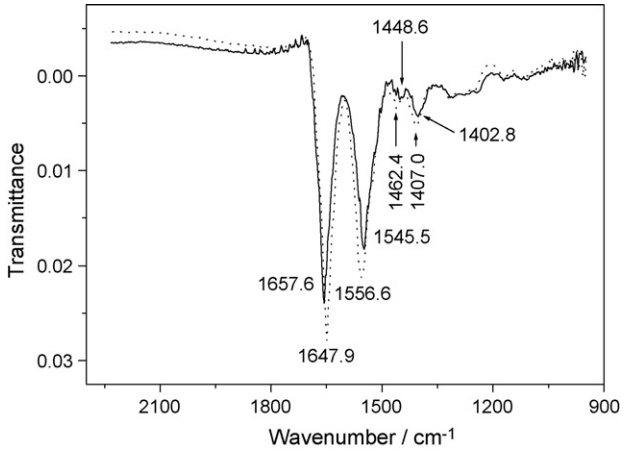

Fig. 5. FT-IR absorption spectra of native Cyt *c* (dotted line) and that of Cyt *c* immobilized on/inside the surface of 3D porous active carbon (solid line).

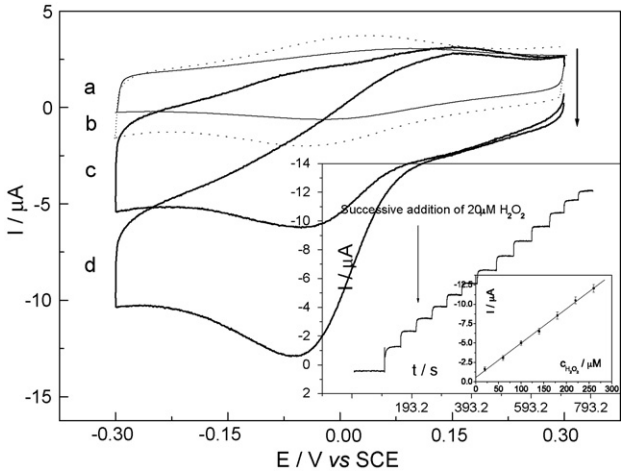

Fig. 6. CV of MPCE in 0.1 mol l^{-1} pH 6.8 PBS containing 30 μmol l^{-1} H_2O_2 (a) and CVs of Cyt *c*/MPCE in 0.1 mol l^{-1} pH 6.8 PBS (b–d) containing 0 (b), 30 (c), and 150 (d) μmol l^{-1} H_2O_2. Scan rates: 0.03 V s^{-1}. Inset: a typical amperometric response to H_2O_2 with successive additions of 20 μmol l^{-1} H_2O_2 at an operating potential of −0.08 V and a stirring speed of 600 rpm. The etched points represent the mean coefficient of variation of five measurements.

The surface coverage (Γ) of Cyt *c* on the surface of MPCE can be determined by integrating the oxidation or reduction peaks of the CV according to $Q = nFA\Gamma$, where Q ($(1.4 \pm 0.1) \times 10^{-7}$) is the charge involved in the reaction, n is the number of electron transferred, F is the Faraday's constant, and A is the electrode area (herein, the geometric area of MPCE is used). This procedure generated the surface coverage of $(2.3 \pm 0.2) \times 10^{-11}$ mol cm^{-2}, which is about 16 times the theoretical monolayer coverage of 1.4×10^{-12} mol cm^{-2} (Dickerson et al., 1971). Obviously, this is because that Cyt *c* is immobilized not only on electrode surface but also inside the 3D porous carbon surface due to the electrostatic and intercalation interactions, and thus the real area involved in immobilizing Cyt *c* is much higher than that of the electrode geometric area, which is employed for the estimation of surface coverage.

3.3. Electrocatalysis of the immobilized Cyt c

Previous results (Lei et al., 1999; Ju et al., 2002) showed that the Cyt *c* "modified" electrodes could display an electrochemical response to hydrogen peroxide (H_2O_2). Here, the electrocatalytic activity of Cyt *c* immobilized on/inside the surface of MPCE to H_2O_2 has also been observed (Fig. 6). As can be seen,

when H_2O_2 was added to solution, the voltammetric behavior of the Cyt *c*-immobilized MPCE changes obviously, with an increase in the reduction peak current and the disappearance of the oxidation peak (curve *c*), and the reduction peak current increases with the increasing concentration of H_2O_2 in solution (curve *d*). However, no obviously direct reduction of H_2O_2 was observed at MPCE in the potential range studied (curve *a*). The disappearance of the oxidation peak shows that the oxidation rate of Cyt *c* by H_2O_2 is very fast, indicating the pseudo peroxidase activity of the Cyt *c* immobilized on/inside the surface of MPCE.

A typical steady-state current response of H_2O_2 is shown in Fig. 6 (inset). As can be seen, the base line of Cyt *c*/MPCE approaches the steady state at nearly the beginning of a run and the background current is 0.51 μA in the sensing system. After adding 20 μmol l^{-1} H_2O_2 in the testing solution, the current response changes from 0.51 to −1.25 μA, and finally reaches equilibrium with a response time of less than 10 s. The response was linear within the H_2O_2 concentration from 2.0×10^{-5} to 2.4×10^{-4} mol l^{-1}. For the regression plot of $i_{p,a}$ versus H_2O_2 concentration, the slope is 0.045 μA/μmol l^{-1}, the *y*-intercept is −0.55 μA and the coefficient of correlation (r^2) is 0.999. The detection limit (3σ) for H_2O_2 is found to be 1.46×10^{-5} mol l^{-1}.

3.4. Reproducibility and stability

To characterize the reproducibility of Cyt *c*/MPCE, repetitive measurements were carried out in 5.0×10^{-5} mol l^{-1} H_2O_2 solution. The results of 11 successive measurements show a relative standard deviation of 3.6%. Also, the modified electrode shows high stability. When the electrode was stored in PBS pH 6.8 at 4 °C in a refrigerator, during the first day the signal decreased by about 2.7% of its initial value, in the next 2 weeks by about 11%, and by about 14% within 1 month.

4. Conclusions

Ordered 3D macroporous active carbon has been fabricated and used as electrode substrate for immobilization and the direct electrochemistry of Cyt *c*. The morphologies and properties of the Cyt *c*/MPCE have been characterized using SEM, FT-IR, and electrochemical techniques. The 3D active carbon electrode leads to good redox behavior of Cyt *c* due to the interaction between the positively charged Cyt *c* and the negatively charged 3D active carbon, which results in the adsorption and intercalation and therefore the immobilization of Cyt *c* on the electrode surface. The Cyt *c* "modified" macroporous active carbon electrode displays the good features of a peroxidase in the electrocatalytic reduction of hydrogen peroxide, and thus can be used as a biosensor for detecting hydrogen peroxide with good reproducibility and stability.

Acknowledgements

The author wishes to acknowledge the financial support of this paper by Shanghai Leading Academic Discipline Project (T0402), Shanghai Municipal Education Commission (05DZ16) and Shanghai Normal University (SK200719).

References

Baizer, M.M., Lund, H., 1983. Organic Electrochemistry. Marcel Dekker, Inc., New York, p. 379 and 507.
Barker, P.D., Gleria, K. Di., Hill, H.A.O., Lowe, V.J., 1990. Eur. J. Biochem. 190 (1), 171–175.
Brabec, V., Bianco, P., Haladjian, J., 1982. Biophys. Chem. 16 (1), 51–59.
Burrows, A.L., Guo, L.H., Hill, H.A.O., McLendon, G., Sherman, F., 1991. Eur. J. Biochem. 202 (2), 543–549.
Cabaniss, G.E., Diamantis, A.A., Murphy, W.R., Linton Jr., R.W., Meyer, T.J., 1985. J. Am. Chem. Soc. 107 (7), 1845–1853.
Collinson, M., Bowden, E.F., Tarlov, M.J., 1992. Langmuir 8 (5), 1247–1250.
Deere, J., Magner, E., Wall, J.G., Hodnett, B.K., 2001. Chem. Commun., 465–466.
Díaz, J.F., Balkus, K.J., 1996. J. Mol. Catal. B: Enzym. 2 (2–3), 115–126.
Dickerson, R.E., Takano, T., Eisenberg, D., Kallai, O.B., Samson, L., Cooper, A., Margoliash, E., 1971. J. Biol. Chem. 246 (5), 1511–1535.
Dimakis, V.T., Gavalas, V.G., Chaniotakis, N.A., 2002. Anal. Chim. Acta 467 (1–2), 217–223.
Eddowes, M.J., Hill, H.A.O., 1977. J. Chem. Soc. Chem. Commun., 771–772.
Feng, Z.Q., Imabayashi, S., Kakiuchi, T., Niki, K., 1995. J. Electroanal. Chem. 394 (1–2), 149–154.
Hagen, W.R., 1989. Eur. J. Biochem. 1829 (3), 523–530.
Han, Y.J., Stucky, G.D., Butler, A., 1999. J. Am. Chem. Soc. 121 (42), 9897–9898.
Hawkridge, F.M., Kuwana, T., 1973. Anal. Chem. 45 (7), 1021–1027.
He, J., Li, X., Evans, D.G., Duan, X., Li, C., 2000. J. Mol. Catal. B: Enzym. 11 (1), 45–53.
Huang, Z.X., Feng, M., Wang, Y.H., Cui, J., Zou, D.S., 1996. J. Electroanal. Chem. 416 (1), 31–40.
Jiang, J.F., Kini, V., Belikova, N., Serinkan, B.F., Borisenko, G.G., Tyurina, Y.Y., Tyurin, V.A., Kagan, V.E., 2004. Lipids 39 (11), 1133–1142.
Jin, W., Wollenberger, U., Schunck, W., Scheller, F.W., 1997. J. Electroanal. Chem. 433 (1–2), 135–139.
Johnson, B.F.G., Raynor, S.A., Shephard, D.S., Mashmeyer, T., Thomas, J.M., Sankar, G., Bromsley, S., Oldmoyd, R., Gladden, L., Mantle, M.D., 1999. Chem. Commun. 13, 1167–1168.
Ju, H., Liu, S., Ge, B., Lisdat, F., Scheller, F.W., 2002. Electroanalysis 14 (2), 141–147.
Laviron, E., 1979. J. Electroanal. Chem. 101 (1), 19–28.
Lei, C., Lisdat, F., Wollenberger, U., Scheller, F.W., 1999. Electroanalysis 11 (4), 274–276.
Lei, Z., Zhang, Y., Wang, H., Ke, Y., Li, J., Li, F., Xing, J., 2001. J. Mater. Chem. 11 (8), 1975–1977.
Liu, Y.U., Cui, S.Q., Yang, Z.S., 2006. Anal. Sci. 22 (8), 1071–1074.
Mattson, J.S., Mark, H.B., 1971. Activated Carbon. Marcel Dekker, New York.
Santucci, R., Faraoni, A., Campanella, L., Tranchida, G., Brunori, M., 1991. Biochem. J. 273, 783–786.
Song, S., Clark, R.A., Bowden, E.F., Tarlov, M.J., 1993. J. Phys. Chem. 97 (24), 6564–6572.
Strauss, E., Thomas, B., Yau, S.T., 2004. Langmuir 20 (20), 8768–8772.
Taniguchi, I., Toyosawa, K., Yamaguchi, H., Yasukouchi, K., 1982. J. Electroanal. Chem. 140 (1), 187–193.
Taniguchi, I., Iseki, M., Yamaguchi, H., Yasukouchi, K., 1984. J. Electroanal. Chem. 175 (1–2), 341–348.
Tarlov, M.J., Bowden, E.F., 1991. J. Am. Chem. Soc. 113 (5), 1847–1849.
Velev, O.D., Kaler, E.W., 2000. Adv. Mater. 12 (7), 531–534.
Wang, J., Li, M., Shi, Z., Li, N., Gu, Z., 2002. Anal. Chem. 74 (9), 1993–1997.
Washmon-Kriel, L., Jimenez, V.L., Balkus, K.J., 2000. J. Mol. Catal. B: Enzym. 10 (5), 453–469.
Wu, Y., Hu, S., 2005. Colloids Surf. B: Biointerfaces 41 (4), 299–304.
Xia, Y., Gate, B., Yin, Y., Lu, Y., 2000. Adv. Mater. 12 (10), 693–713.
Yablonovitch, E., 1987. Phys. Rev. Lett. 58 (20), 2059–2062.
Zhao, G.C., Yin, Z.Z., Wei, X.W., 2005. Front. Biosci. 10 (1), 2005–2010.